A robust method for quantifying the contribution of transient dynamics to variation in population growth rate

Christina M. Hernández*[1,†], Harman Jaggi[2,†], James Cant[1], Wenyun Zuo[3], Shripad Tuljapurkar[3,‡], and Roberto Salguero-Gómez[1, ‡]

[1]University of Oxford, Department of Biology, South Parks Road, Oxford OX1 3RB, UK
[2]Princeton University, Ecology and Evolutionary Biology, NJ, 08540, USA
[3]Stanford University, Department of Biology, CA, 94305, USA
[†]Co-first-authors; These authors contributed equally.
[‡]Co-senior-authors; These authors contributed equally.

March 20, 2026

A manuscript for preprinting at EcoEvoRxiv before peer review.

Data availability statement The data that support the findings of this study are openly available at www.compadre-db.org. All code files required to repeat the analyses are archived at Zenodo (https://doi.org/10.5281/zenodo.19093535).

*Corresponding author. Current address: Department of Biological Sciences, Old Dominion University, Norfolk, Virginia, USA. Email: cmhernan@odu.edu

Abstract

Understanding why population growth rates vary through time is central to ecology, evolution, and conservation. In structured populations, such variation arises from both environmentally-driven fluctuations in vital rates and intrinsic transient dynamics generated by changes in population structure. Despite long-standing recognition of these processes, existing approaches do not provide an exact and general partitioning of their relative contributions. Here, we develop a mathematically rigorous framework that decomposes variation in realized population growth rate into contributions from fluctuations in vital rates and from transient deviations in population structure. Building on stochastic population theory, we derive a first-order decomposition under stationary environmental variation, yielding analytical expressions for the variance components associated with each source. This framework clarifies how damping rate, life-history speed, and covariance among vital rates shape temporal variability in growth. We complement the analytical results with a simulation-based procedure that allows the decomposition to be estimated from time series of population projection matrices without requiring observations of past population structure. Applying the method to empirical case studies spanning plants and animals with contrasting generation times, we show that short-lived species exhibit variability dominated by vital-rate fluctuations, whereas long-lived species can exhibit substantial contributions from transient population structure when vital-rate variation is sufficiently large. Our approach provides a unifying and exact link between stochastic demography and transient dynamics, offering a powerful tool for comparing life histories, testing ecological hypotheses, and evaluating how environmental variability propagates through population structure to influence population growth.

Keywords: convergence, matrix population models, population structure, stochastic demography, short-term dynamics, variance decomposition.

1 Introduction

Population growth rate underpins many ecological and evolutionary processes, with key implications for the conservation of wild populations (Sibly and Hone, 2002). For instance, population growth rate is often considered a proxy measure for the average fitness of a population (Crone et al., 2011; Metz et al., 1992), and invasion growth rates are commonly used to understand coexistence (Godoy and Levine, 2014). Ecosystem management efforts, both in terms of conservation (Hone et al., 2010) and pest management (Thomas, 1999) also focus on setting population growth rate to a target level (Koons et al., 2006; Sutherland and Norris, 2002). As such, an important and long-standing question is: what factors drive variation in population growth rate?

In demographic models, variation in population growth rate can be generated by both extrinsic and intrinsic dynamics. In these models, individuals are structured by age, size, and/or stage (simply "stage" hereafter), according to how an individual's stage affects their probability of survival or reproductive output (Caswell, 2001; Ellner et al., 2016). By extrinsic dynamics, we refer to the possible ways that survival, growth, and reproduction can be impacted by temporal variation in the environment—this could be related to abiotic (*e.g.*, Lindell et al., 2022; Oldfather and Ackerly, 2019; Paniw et al., 2021) or biotic (*e.g.*, Greenberg and Green, 2013; Rudgers and Hoeksema, 2003) factors. By intrinsic dynamics, we refer to the fact that variation in population structure can generate fluctuations in population growth rate, even if vital rates are constant (Stott et al., 2011). This propensity of a structured population model to generate its own fluctuations, and the study of these processes and their consequences, such as deviating from long-term projections, is referred to as transient dynamics (Hastings, 2004; Jaggi et al., 2025; Stott et al., 2011).

In a structured population model, these intrinsic and extrinsic drivers are linked to one another through the population structure, the proportional distribution of the population stages. Most matrix population models that have been built for plants and animals are ergodic, meaning that their long-term behavior is independent of their initial conditions (Stott et al., 2010; Tuljapurkar, 1990). Due to this ergodicity, if conditions were constant across time, population size would eventually grow or shrink at a constant exponential rate (Caswell, 2001, page 79-92). From then on, the population structure would also remain constant while popu-

lation size increases or declines. However, when (a)biotic conditions—and, as a consequence, vital rates—change across time, the population growth rate varies from year to year without converging to a constant value.

The variation in population growth rate can be separated into contributions from two sources (Tuljapurkar, 1990). The first, and more obvious source, is the immediate effect that changes in the environment have on changes in vital rates of survival, growth, and fecundity. For instance, in a bad year for reproduction, population growth rate will tend to be lower than in a year that is good for reproduction. The second, perhaps less obvious source, is the effect of the population structure on population growth rate. For example, if population structure is concentrated in non-reproductive classes, then the (one-step-ahead) population growth rate will tend to be lower than if the population structure were concentrated in reproductive classes. When vital rates vary through time, the population structure also varies—low reproductive output at time 1 will lead to a low relative frequency of young individuals at time 2. Therefore, the population structure at a specific time results from the accumulated effects of a population's history of variation in vital rates. Moreover, that variation in population structure has its own effect on realized population growth rate independent of any vital rate effects[1]. In past work, the effect of variation in population structure on realized population growth rate has been referred to as 'transient growth' (Hastings et al., 2018; McDonald et al., 2016). So, we might ask, what is the relative importance of vital rates and population structure in driving variation in population growth rate?

Demographers have developed a rich toolbox of methods for analyzing variation in population growth rate for structured population models. For example, sensitivity and elasticity analyses quantify the effect on population growth rate of changes in vital rates (De Kroon et al., 2000; Heppell et al., 2000). Said metrics can be applied to models that are deterministic (Caswell, 2007; Caswell, 2019) or stochastic (Haridas and Tuljapurkar, 2005; Kajin et al., 2025; Tuljapurkar et al., 2003). Life Table Response Experiments (LTREs) decompose the deviance or variance in population growth rate between/among empirical population models into the contributions from various vital rates (Caswell, 1989; Hernández et al., 2023; Knape et al., 2023; Koons et al., 2016). However, most of these approaches do not allow us to distinguish between the effect of immediate changes in vital rates from the accumulated effects of

[1] We assume variation in vital rates is independent of population density.

historical variation in vital rates. Transient LTRE (Koons et al., 2016) does provide a method for decomposing the variance in population growth rate into contributions from vital rates and population structure, but its data requirements have thus far limited its applications (but see Dobson et al. 2024; Knape et al. 2023; Maldonado-Chaparro et al. 2018; Summers et al. 2024). Transient LTRE is a retrospective analysis of the observed population dynamics that requires a complete time series of vital rates, population structure, and realized population growth rate (Koons et al., 2016). Conversely, stochastic population theory is based on a view of environmental variation wherein repeated observations of vital rates are samples from a stationary noisy process that may or may not include autocorrelation (Jaggi et al., 2024a; Robey et al., 2025; Tuljapurkar and Haridas, 2006).

Here, we focus on this stochastic view of the environmentally-driven variation in vital rates because it does not require observation of past population structure. Instead, we can look at temporally-replicated observations of vital rates (*e.g.*, matrix population models) and assume that they are random samples from a stationary distribution of vital rate combinations arising from different environmental states. Based on this same framework of stochastic variation in vital rates, past research used correlation approaches to decompose variation in population growth rate, showing that the contributions from variation in population structure is important in plants (Ellis and Crone, 2013; McDonald et al., 2016). Here, we build on the work of McDonald et al. (2016) and Ellis and Crone (2013) by developing a mathematically complete and exact decomposition of population growth rate into contributions from vital rates and contributions from population structure. We first introduce the mathematical decomposition of variance. Next, we discuss several analytical insights that emerge from the approach. Finally, we explore a few case studies to demonstrate the ecological interpretation of results and whether they match the analytical expectations.

2 Methods

In this section, we introduce the time-varying population model and the decomposition of the population growth rate into the effects of changes in vital rates and population structure. To understand the influence of fluctuations in vital rates and population structure on population growth rate, we decompose the variance in population growth rates into contributions from

variance in vital rates and variance in population structure. We then derive analytical expressions for those contribution terms and discuss the implications of those analytical results. Finally, we present a simulation approach to compute the decomposition for any time series of matrix population models. Our notation is summarized in Table 2.

2.1 Population model

We first imagine an ideal scenario where we have an infinitely long series of population projection matrices ($\mathbf{A}_t$), each representing the vital rates applying to the transition between a subsequent pair of annual censuses. We model the population dynamics with a time-varying projection matrix $\mathbf{A}_t$ such that:

$$\mathbf{A}_t = \overline{\mathbf{A}} + \epsilon \mathbf{H}_t, \text{ with } \mathcal{E}[\mathbf{H}_t] = 0. \tag{1}$$

Here, $\overline{\mathbf{A}}$ is the mean projection matrix and $\mathbf{H}_t$ is the perturbation matrix, such that each element $h_{ij,t}$ represents the deviation at time t from the mean value of the vital rate in $\overline{\mathbf{A}}$. Thus, the population matrix at time t can be written as a decomposition of the mean model $\overline{\mathbf{A}}$ (the average over the infinitely long time series) and the random perturbations to its underlying vital rates (*e.g.*, survival, reproduction) $\mathbf{H}_t$. By including the factor ϵ, we indicate our assumption that the perturbations are sufficiently small to allow certain mathematical approximations. Specifically, this assumption allows us to ignore any terms of order ϵ^2 or higher—if ϵ is much smaller than 1, the value becomes vanishingly small as it is raised to powers of 2, 3, 4.

By definition, the expected values (*i.e.*, the average over the infinitely-long time series) of the perturbations must be equal to 0, or else they would cause the entries of the mean matrix to change. The dominant eigenvalue of the average matrix $\overline{\mathbf{A}}$ is λ_d, with corresponding normalized right eigenvector $\mathbf{u}$. Meanwhile, we refer to the realized population growth rate as λ_t, which is the ratio of population size at time t over population size at time $t-1$.

Let $\mathbf{w}_t$ denote the population structure at time t. The projection matrix $\mathbf{A}_t$ applies between $t-1$ and t, and maps the stage structure at the beginning of the time interval

$(t-1, t)$ to $\mathbf{w}_t$. The population structure at time t is

$$\mathbf{w}_t = \frac{\mathbf{A}_t\, \mathbf{w}_{t-1}}{\lambda_t}, \quad \lambda_t = (\mathbf{e}, \mathbf{A}_t \mathbf{w}_{t-1}), \tag{2}$$

The population structure is expressed as the proportion of individuals in each class, so the structure always sums to 1, *i.e.*, $(\mathbf{e}, \mathbf{w}_t) = 1$, where $\mathbf{e}$ is a vector of ones and $(\cdot, \cdot)$ indicates a scalar product between two vectors.

Just as we decomposed the projection matrix ($\mathbf{A}_t$), we decompose the population structure $\mathbf{w}_t$ as follows:

$$\mathbf{w}_t = \overline{\mathbf{w}} + \epsilon \mathbf{z}_t, \tag{3}$$

where $\overline{\mathbf{w}}$ is the average (long-term) stage distribution and $\mathbf{z}_t$ is the deviation of the population structure from $\overline{\mathbf{w}}$ at time t. Because stage structure is expressed as proportions, the sum of the deviations of the structure must sum to 0 (an increase in one stage class relative to $\overline{\mathbf{w}}$ must be balanced by a decrease in another stage class), hence $(\mathbf{e}, \mathbf{z}_t) = 0$. In the limit where perturbations are small ($\epsilon \to 0$), $\overline{\mathbf{w}}$ is equivalent to the stable stage distribution (right eigenvector) associated with the mean matrix $\overline{\mathbf{A}}$.

We define the scaled projection matrix $\mathbf{B}_t = \frac{\mathbf{A}_t}{\lambda_d}$ and the scaled fluctuations $\mathbf{G}_t = \frac{\mathbf{H}_t}{\lambda_d}$ and work with these scaled matrices from here onwards. Note that, given this scaling:

$$\frac{\mathbf{A}_t}{\lambda_d} = \mathbf{B}_t + \epsilon \mathbf{G}_t \tag{4}$$

2.2 Decomposing realized population growth rate

In structured populations, changes in abundance over time can be influenced by (1) how individuals are distributed across stages, and (2) how vital rates (survival, growth, reproduction) vary over time. To separate these effects, we decompose the realized population growth rate λ_t into contributions from the mean long-run growth rate and from first-order fluctuations in population structure and vital rates. The derivation is given in Appendix S2 and S4. The population growth rate can be expanded as

$$\boxed{\lambda_t \;=\; \lambda_d + \epsilon\, \Delta_Z + \epsilon\, \Delta_R} \tag{5}$$

where

- λ_d is the asymptotic growth rate of the mean projection matrix $\overline{\mathbf{A}}$, given by its dominant eigenvalue,
- $\Delta_Z = \lambda_d\left(\mathbf{e}, \mathbf{B}\mathbf{z}_{t-1}\right)$ represents the effect of mean vital rates acting on fluctuations in population structure,
- $\Delta_R = \lambda_d\left(\mathbf{e}, \mathbf{G}_t\mathbf{u}\right)$ represents the effect of fluctuations in vital rates acting on the mean population structure,

Ecologically, this means that deviations in the one-step-ahead population growth rate λ_t from the long-term mean growth rate λ_d can occur either because the population structure is away from its stable state distribution or because of variability in vital rates such as survival or reproduction. Here, we will assume that the effects of interactions between vital rates and structure are very small (if we fully expanded the expression in Equation (S13), the interaction term would have a leading factor of ϵ^2).

2.3 Expectation and variance

If we assume that the population has been increasing according to the model described by Equation (1) for a long time T and that our models are ergodic, then the time-average of a given population metric (*e.g.*, population growth rate, vital rates) is equal to its expectation. Since we previously defined the expected value of perturbations to be 0 ($\mathcal{E}[\mathbf{H}_t] = 0$ and $\mathcal{E}[\mathbf{G}_t] = 0$), we can assume that the time-averaged vital rate perturbations are also effectively 0. In turn, this assumption implies that the average magnitude of the effect of vital rate perturbations acting on mean population structure $\mathcal{E}[\Delta_R]$ is 0. Likewise, when the expected value of the population structure is equal to its time-average, Equation (3) implies that the expected value of the population structure perturbations $\mathbf{z}_t$ must be 0.

Therefore, from Equation (5), we find that the expected value of λ_t is equal to λ_d, the dominant eigenvalue of our time-averaged projection matrix $\overline{\mathbf{A}}$. And, finally, we arrive at an expression for the variance in population growth rate as the sum of the contributions from variance in population structure ($\mathrm{Var}(\Delta_Z)$) and contributions from variance in vital rates ($\mathrm{Var}(\Delta_R)$).

$$\boxed{\mathrm{Var}\lambda_t = \epsilon^2\mathrm{Var}(\Delta_Z) + \epsilon^2\mathrm{Var}(\Delta_R)} \tag{6}$$

The first term $\mathrm{Var}(\Delta_Z)$ corresponds to variance due to deviations in population structure from its stable stage distribution ($\mathbf{u}$). Because these deviations are generated by past fluctuations in vital rates, this term reflects how much demographic memory (*sensu* (Jaggi et al., 2025; Tuljapurkar and Haridas, 2006)) the system has. More specifically, this term reflects the importance of transient dynamics—how responsive the system is to fluctuations and how quickly those responses decay. The second term $\mathrm{Var}(\Delta_R)$ corresponds to variance generated by fluctuations in the vital rates. Since this term depends on the random perturbation matrix $\mathbf{G}_t$ acting on the mean population structure $\mathbf{u}$, $\mathrm{Var}(\Delta_R)$ captures the effect of variability in survival, growth, or reproduction at time t, independent of transient effects of population structure. Together, these terms describe how variation arises both from extrinsic variation in vital rates and from intrinsic demographic memory.

2.4 Linking analytical results to ecological implications

In this section, we will briefly discuss the model components that drive the variance terms and the ecological implications. In Appendix S4, we provide the full derivations of analytical expressions for the variance terms $\mathrm{Var}(\Delta_Z)$ and $\mathrm{Var}(\Delta_R)$.

Our analytical results imply that the *contribution from variance in vital rates*, $\mathrm{Var}(\Delta_R)$, depends on how the life history of the population interacts with environmental variation. Mathematically, the contribution from variance in vital rates is given by the product of the variance-covariance matrix of vital rate perturbations ($\mathcal{E}[\mathbf{H}_t \otimes \mathbf{H}_t]$) and the stable population structure ($\mathbf{u}$). In other words, the contribution from variance in vital rates is the sum of the variance in vital rates, weighted by the stable distribution. Ecologically, this means that the contributions of fluctuations in vital rates will be highest if there is high variance in vital rates corresponding to stages that are prevalent in the stable stage distribution. For example, if germination rate is highly variable and the population structure is strongly skewed towards seeds, then we would see a high contribution from Δ_R.

In the case of the *contribution from variance in population structure*, $\mathrm{Var}(\Delta_Z)$, the story is a little bit more complicated. Mathematically, this contribution term is proportional to the product of the mean vital rates ($\overline{\mathbf{A}}$) and the variance-covariance matrix of fluctuations in population structure ($\mathcal{E}[\mathbf{z}_t \otimes \mathbf{z}_t]$). The variance-covariance matrix of fluctuations in population structure is itself a product of the variance-covariance matrix of vital rates, the stable popula-

tion structure, and the transient portion of the population matrix (Equation S45). Therefore, the contributions from variance in population structure will be highest in models where the transient dynamics decay slowly. Remember that, in our model, the variation in population structure is generated by the perturbations to vital rates that occurred in past time steps. So, populations with more excitable population structure or with more "memory" for these past vital rate perturbations will show a greater contribution from Δ_Z. Because convergence rate is inversely proportional to generation time (Jiang et al., 2022), we would expect greater contributions from variance in population structure in long-lived and late-maturing species.

These analytical results also underscore the importance of covariances between vital rates in driving the overall variance in population growth rate. Both variance contribution terms depend ultimately on the variance-covariance matrix of vital rate perturbations. Therefore, both contribution terms—and, by extension, overall variance in population growth rate—can be minimized if there are negative covariances between vital rates. If good years for survival are bad years for fecundity and *vice versa*, then the fluctuations in population growth rate will be small. The damping effect of these negative covariances among vital rates are mediated through both the contributions of variance in vital rates and the contributions of variance in population structure.

In light of these analytical results, we can make some predictions about which life history strategies should exhibit variation in population growth rate dominated by contributions from vital rates *vs.* contributions from structure. Species with a fast life history tend to have population structures skewed towards small, vulnerable stages and to exhibit higher variance in survival than reproduction. As such, we would expect them to exhibit relatively high variation in population growth rate with the contributions from vital rates dominating. Meanwhile, species with a slow life history tend to have populations with more even distributions across young and old individuals (but reproductive strategy can be important here, *e.g.*, fish and trees). Furthermore, species with long generation time should exhibit more "memory" of past vital rate perturbations, meaning that we expect their variation in population growth rate to be dominated by contributions from population structure.

3 Using simulations to decompose growth rate

To numerically calculate the terms in the decomposition of variance in population growth rate into the contributions shown in Equation (6), we use a simulation procedure. For each simulation, we use an initial population vector that is evenly distributed across classes. To remove any effects of this initial population vector, we use a burn-in period, *i.e.*, simulation time steps that are discarded before calculating the decomposition. We recommend a burn-in time of $100T_g$, where T_g is the generation time. This period is sufficiently long to remove any effects of the initial population vector. The decomposition is then calculated for one time step following the burn-in.

This step should be repeated for a large number of replicates. We recommend 500 replicate runs. For each replicate run, we saved the projection matrix for the final time step ($\mathbf{A}_t$), the population structure at the start of the final time step ($\mathbf{w}_{t-1}$) and the realized population growth rate for the final time step ($\lambda_t = (\mathbf{e}, \mathbf{A}_t\mathbf{w}_{t-1})$). For a detailed explanation of our simulation algorithm, see Supplemental Section S7 or the supplemental code.

4 Case studies

To demonstrate the application of both our analytical and simulation methods, as well as interpretation of the results, we present several case studies. We selected these case studies from the COMADRE and COMPADRE databases of matrix population models from animals and plants, respectively (Salguero-Gómez et al., 2015; Salguero-Gómez et al., 2016). First, we filtered the 3,488 and 8,994 matrices in COMADRE (v4.23.2.1) and COMPADRE (v6.23.5.0), respectively, for matrices that represented natural populations under unmanipulated conditions. To focus on populations with the ability to exhibit transient dynamics, we excluded any studies where the life cycle was represented with fewer than three stages. We required that these matrices were separable into survival transitions among classes ($\mathbf{U}$ matrix), and reproduction ($\mathbf{F}$ matrix) so that we could calculate generation time using the definition of Bienvenu and Legendre (2015). We also required that sexual reproduction was observed/included in the study design, and we excluded models with clonal reproduction. We removed any matrices with impossible survival values, *i.e.*, any columns in the $\mathbf{U}$ matrix with a column sum greater than 1.001. We then restricted our subset to studies that contained at

Table 1: Information on case studies. All matrix population models have a time step of one year. Generation time (T_g) is measured in years. Population growth rate (λ_d) refers to the eigenvalue of the mean matrix $\overline{\mathbf{A}}$.

Species	**Common name**	**Reference**	T_g	**N matrices**	λ_d
Orcinus orca	Orca	Vélez-Espino et al. (2014)	32	24	0.989
Actaea spicata	Baneberry	Fröborg and Eriksson (2003)	17	6	0.975
Dicerandra frutescens	Scrub mint	Menges et al. (2006)	16	9	0.838
Callospermophilus lateralis	Golden-mantled ground squirrel	Hostetler et al. (2012)	1	18	2.05

least four matrices for the same species. These selection criteria left us with 472 and 1,981 matrices from 29 and 144 species for animals and plants, respectively.

Next, we manually inspected these sets to identify groups of matrices that pertained to temporal replication at the same population or geographical site. Our manually-screened sets of matrices are given in the archived data files `comadre_ScreenedMatrixSets.csv` and `compadre_ScreenedMatrixSets.csv` for animals and plants, respectively. From those possible populations, we selected a few that cover a range of generation times, with preference for particularly long time series. The details of the populations we selected are given in Table 1 and each study is briefly introduced along with biological interpretation of the results.

We first illustrate the importance of incorporating population structure in the Appendix figures S.1. In our examples, we compare structured matrix population models with corresponding unstructured models (obtained by collapsing each annual matrix to a single survival and fertility rate) for three of our case study species: baneberry, scrub mint, and ground squirrels. Details of the case studies are provided in Table 1 and in sections 4.2, 4.3, and 4.4 below. We find that even though both models experience the same sequence of environmental variation, the model without population structure can produce inaccurate estimates of both population size and growth rate. This is because ignoring structure omits demographic memory and transient effects. The comparison highlights that variation in population growth rate is not driven by vital rates alone, but also by the stage structure on which those rates act.

4.1 Orcas

Orcas (*Orcinus orca*) are a long-lived marine mammal and a top predator in the ocean. The study was carried out on two populations of "resident killer whales" in the Northeast Pacific Ocean, near the border between the United States and Canada (Vélez-Espino et al., 2014).

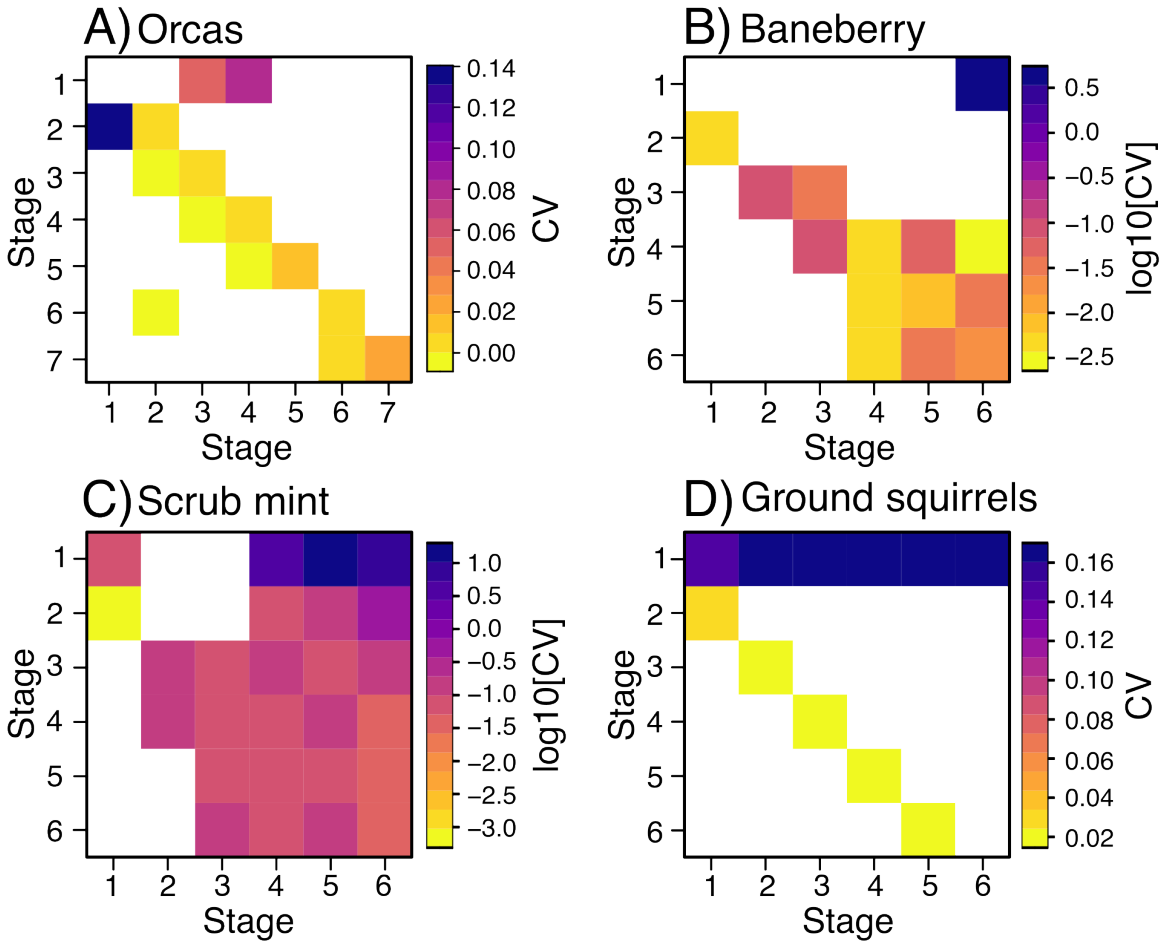

Figure 1: The four case studies show distinct patterns of variation in matrix elements. In each panel, the grid of boxes indicates the elements of the population projection matrix. The grid is colored according to the coefficient of variation for each matrix element across the time series of matrices. Note that the color scale is log-transformed for (B) baneberry and (C) scrub mint, but not for (A) orcas or (D) ground squirrels.

For both the northern and southern populations, there are 24 annual transition matrices. The life cycle was represented by a two-sex model with seven life stages: calves and juveniles (both sexes), two stages of mature males (young and old), and three stages of females (young reproductive, old reproductive, and post-reproductive). Here, we examine the southern population, which has a generation time of 32 years and an asymptotic population growth rate indicating slight declines in the long term ($\lambda_d = 0.989$).

In the orca population, the variation in vital rates is quite small, with coefficients of variation below 10% for all vital rates except calf survival, which has a CV of 13% (Figure 1A). As a result, the variance in population growth rate is very small ($\mathrm{Var}\lambda_t = 0.0013$). In contrast to our expectation (based on the analytical results) that long-lived species should have

more contributions from variation in population structure, the small variation in population growth rate for these orcas is almost entirely due to variation in rates (Figure 2A). A plausible explanation for this result is that the variation in vital rates was too small in this case to excite the population structure such that transient dynamics persist over multiple time steps.

4.2 Baneberry

Baneberry (*Actaea spicata*) is a perennial understory herb. The populations studied by Fröborg and Eriksson (2003) were in southeastern Sweden—one in a deciduous forest and one in a mixed coniferous forest. Both populations were studied for seven years, yielding six transition matrices. The model represents the baneberry life cycle with six stages: seed, seedling, juvenile, small vegetative, large vegetative, and reproductive. The population that we focused on for the case study is from the deciduous forest site. This population has a generation time of 17 years, and the long-term population growth rate for the mean matrix is 0.975 (Table 1), indicating a declining population.

Most of the vital rates show a very small variation across years, with the exception of seed production, which has a CV of 342% (Figure 1B). The analytical and simulated results agree quite well, with vital rates and population structure each contributing approximately half of the variance in population growth rate (Figure 2B). Here, unlike with the orcas, the variation in vital rates (perhaps specifically variation in seed production) is large enough to generate perturbations to population structure that persist due to the long generation time.

4.3 Scrub mint

The endemic Florida scrub mint (*Dicerandra frutescens*) is an endangered herbaceous perennial found in fire-prone scrub environments. The study that included our focal population investigated the optimal fire return interval for the viability of this species in Florida shrubland (Menges et al., 2006). The authors used matrix population models with six life stages: a persistent seedbank, seedlings, vegetative individuals and three sizes of flowering individuals (small, medium, and large). The authors found that in the absence of fire, populations of scrub mint would decline.

Because we are interested here in variable environments without serial autocorrelation, we considered a population in a habitat site that had not experienced fire in a long time

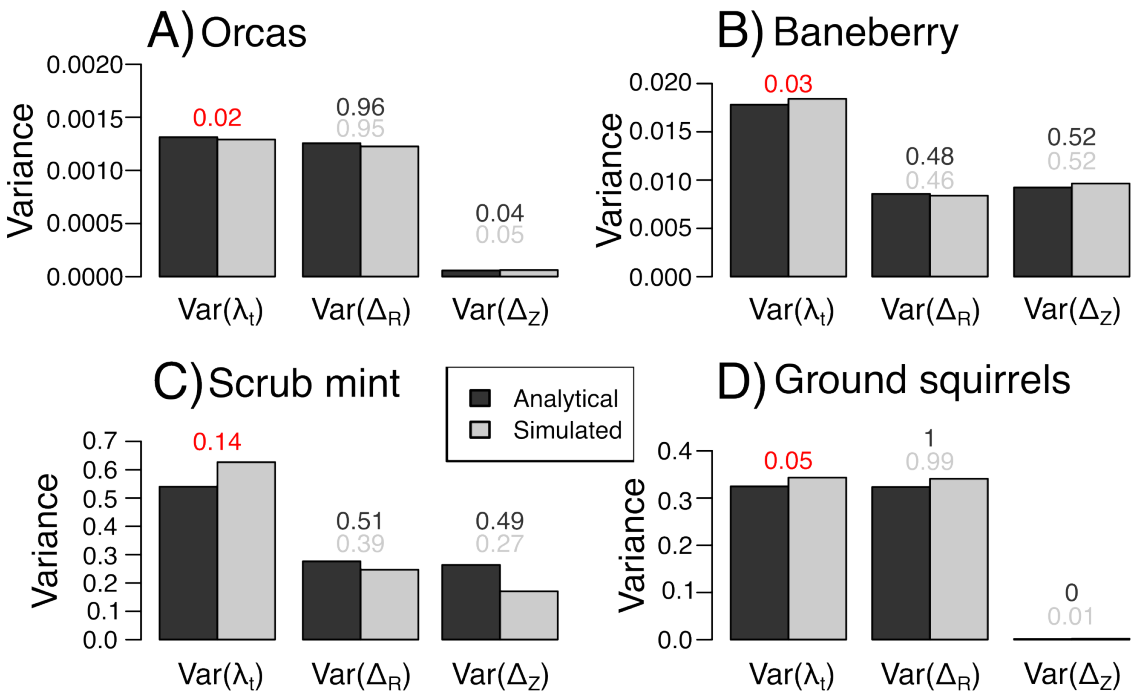

Figure 2: Decomposition of variance in population growth rate for the case studies. Each panel represents one case study, and shows the comparison between the analytical and simulation results for variance in λ_t, the contribution from variance in Δ_R, and the contribution from variance in Δ_Z. Note that y-axis limits differ among panels. Analytical terms are as given in Equations 6, S41, and S62, while simulated terms are calculated directly from the simulations. The red number indicates the percent error between the analytical and simulated value of variance in λ_t (treating the simulation as correct because the analytical result neglects any possible interaction terms). The grey numbers above the $var(\Delta_R)$ and $var(\Delta_Z)$ bars indicate the proportion of $var(\lambda_t)$ that is explained by each of the components.

and did not experience fire during the study interval. The population that we analyze here, Population 4 in a sand pine scrub habitat site, was monitored starting in 1988 and was in a "long-unburned" state until 1998, yielding nine transition matrices for our simulations. Taking the mean matrix of these nine years implies that the population had a generation time of 16 years and long-term population growth rate of 0.838 (Table 1).

The matrices for scrub mint (Figure 1C) exhibit high variation in the production of seeds (CV range 355 to 1048%), and moderate values of variation in production of seedlings (CV range 7 to 60%) and the matrix entries related to survival and transitions among the various adult stages (CV range 3 to 19%). As the result of this variation in vital rates, the variation in population growth rate is markedly higher than for the orcas or baneberry cases. Furthermore, the analytical results do not match the simulation results that closely (14% error, Figure 2C). Surprisingly, the simulations have a higher total value of variance in population growth rate, but lower values of both contribution terms. This result suggests that, despite our simulations being run as uncorrelated random environments, there are sizable interaction terms arising from covariance of vital rates and population structure. According to the simulation results, interactions may contribute as much as 44% of the overall variance in population growth rates.

4.4 Ground squirrels

The golden-mantled ground squirrel (*Callospermophilus lateralis*) is a small striped ground squirrel that is widely distributed in western North America. A population at the Rocky Mountain Biological Laboratory in Colorado, USA was monitored with 19 annual censuses between 1990-2008 (Hostetler et al., 2012). From these data, the authors built 18 annual transition models. The age-based transition matrices have six classes, from young of the year up to six years old, with no survival for six-year-old individuals. Juveniles are able to reproduce in their first year, and survival is fairly low, such that the generation time is one year.

In this population, the vital rates and population growth rate show moderate interannual variation (Figure 1D). In particular, reproductive output has a CV of 16%, while survival parameters show much smaller variation with a CV of 2.4%. Still, this variation leads to fairly high variance in population growth rate compared to the other case studies (Figure 2). However, it is worth noting here that the asymptotic population growth rate for the

mean matrix ($\overline{\mathbf{A}}$) is more than double the value for the other case studies (λ_d=2.05). Still, in this short-lived species that has a generation time of approximately 1 year, the variance in population growth rate is exclusively due to variation in vital rates, with no contributions from structure. This matches our expectation due to their extremely short generation time, that transient dynamics (*i.e.*, fluctuations in population structure due to past variation in vital rates) decay extremely quickly and therefore do not contribute to variance in population growth rate.

5 Discussion

Population ecology fundamentally seeks to identify and understand the drivers of variation in population growth rate across time, space, and the Tree of Life (Sutherland et al., 2013). Variation across time is particularly important, because it can be generated by many processes, including environmental variability (Houston and McNamara, 1990; Vázquez et al., 2017), biotic interactions (Levine et al., 2024), transient perturbations (Jaggi et al., 2025; Wiedenmann et al., 2009), or interactions of these (*e.g.*, Coulson et al., 2001). Here, we focus on environmentally-driven variation in vital rates and the propensity of the population to "remember" past vital rate variation through transient fluctuations in population structure. We present a simple, robust framework for decomposing variation in population growth rate into contributions from variation in vital rates and contributions from variation in population structure. When we assume that the vital rates are drawn from a stationary distribution of possible environments, without any auto-correlation, we can derive analytical results that predict when the contribution from vital rates or population structure should be greatest. The contribution of vital rate fluctuations to population growth rate will be highest when there is high variation in vital rates corresponding to dominant stages in the population structure. Meanwhile, variation in population structure will be greatest in populations with long generation time, where transient dynamics decay slowly. Our four case studies generally match these expectations, while also highlighting the importance of the magnitude of variation in vital rates.

We illustrate the importance of accounting for population structure by comparing structured and unstructured models. We find ignoring population structure produces inaccurate

and biased estimates of both population size and growth rate. Past work has developed non-exact approaches to decompose variation in population growth rate into contributions from vital rates and contributions from population structure. For example, Ellis and Crone (2013) decomposed the population growth rate in a given time step into the asymptotic and transient components. Their approach is distinct from that presented here in that they do not conceive of the vital rates as being perturbed from a mean value, but rather they define the contribution of vital rates as the asymptotic population growth rate in a given time step (*i.e.*, eigenvalue of $\mathbf{A}_t$). Therefore, although they use a similar simulation procedure to ours, they define the variance contributions as the pairwise correlations among realized population growth rate ($r_t = \log \lambda_t$), the contributions of vital rates, and the contributions of transient dynamics (Ellis and Crone, 2013). In both Ellis and Crone (2013) and a follow-up study using a larger dataset of matrix population models for plants, transient dynamics contributed, on average, more than 50% of the variation in population growth rate (Ellis and Crone, 2013; McDonald et al., 2016). However, it is important to note that this correlation method is not exact: the relative contributions of asymptotic dynamics, transient dynamics, and their interaction does not always sum to 100%. In contrast, our approach is exact because the mathematical decomposition of variance is derived directly from the definition of the stochastic population model. As such, we present both analytical and simulation-based results, which generally agree well.

A promising approach for variance decomposition in temporally-variable structured population models is the transient Life Table Response Experiment (transient LTRE; Koons et al. 2016). Transient LTREs are a *retrospective* method, wherein a time series of past vital rates and population structure can be decomposed to understand contributions of specific vital rates, population structure, and their interactions (Cant et al., 2025; Koons et al., 2016). An important extension of the transient LTRE approach further relates vital rates to environmental covariates (Knape et al., 2023). This extension enables the quantification of contributions from demographic stochasticity, defined as a mismatch between realized vital rates and those expected based on environmental covariates (Dobson et al., 2024). Past work using transient LTREs has found an important role for demographic stochasticity (23 or 56%) while population structure contributed less than 5% of variation in population growth rate (Dobson et al., 2024; Knape et al., 2023). Both of these studies are on small populations (10-120 individuals

of a single sex) of relatively short-lived (generation time 2-5 years) species. These results are not surprising in light of the small population size and our analytical results that predict smaller contributions from population structure in short-lived species.

Our method is a valuable complement to transient LTRE analyses for decomposing variation in population growth rate. An important advantage of the transient LTRE method is that it does not require any assumptions about the distribution of environmental states. Meanwhile, our analytical results assume that the vital rates are drawn from a stationary distribution of environmental states, and our simulation results require long burn-in periods with a specified sampling distribution of environmental states. On the other hand, transient LTRE requires complete information on past states (*i.e.*, a time series of vital rates and population structure), while our method requires only temporally-replicated observations of vital rates. Furthermore, our method is better suited to explore hypotheses about the relative importance of transient dynamics under different environmental scenarios (*e.g.*, climate change, different disturbance return intervals, management strategies) or for different life history strategies.

One of the limitations in the analytical framework is that we assume the long-run expectation of perturbation to vital rates is 0 ($\mathcal{E}[\mathbf{H}_t]$ or $\mathcal{E}[\mathbf{G}_t]$). This means that environmental perturbations fluctuate around a stationary mean and that there is no directional trend such as warming (Johnson and Lyman, 2020) or increased drought frequency (Chiang et al., 2021), among others. Thus, the average projection matrix $\overline{\mathbf{A}}$ captures the mean demographic regime, and fluctuations are expressed through Δ_R and Δ_Z. This is a common assumption in stochastic demography and holds for systems that exhibit interannual variability with no sustained trends (Tuljapurkar, 1990). The assumption also implies that the time-average of vital rate perturbations can be approximated by the expectation, which requires sufficiently long time-series (Tuljapurkar, 1990). Further research can examine what happens when vital rate perturbations are temporally autocorrelated. Autocorrelated time series have 'memory' such that population sizes are negatively or positively correlated with past population sizes (Pilowsky and Dahlgren, 2020; Tuljapurkar and Haridas, 2006). Positive autocorrelation leads to sequences of "good" or "bad" years becoming longer whereas negative autocorrelation leads to alternating conditions, preventing long runs of favorable or unfavorable environments. In our framework, incorporating temporal autocorrelation does not change the decomposition for population growth rate in Eq. (4) but changes the variance equations. Recent studies

(Francis et al., 2021; Morozov et al., 2024) have also highlighted the importance of 'long transients' that can last for hundreds of generations or even longer, and is another avenue for future research.

In examples where we find low variance in population growth rate ($\mathrm{Var}(\lambda_t) \approx 10^{-3}$ as in the orca case study), it is important to question whether there is a true signal or a result of parameter uncertainty. Recent research in demography has emphasized a lack of standardized protocol for uncertainty quantification, propagation, and reporting for matrix population models (Gascoigne et al., 2023; Simmonds and Jones, 2024). Indeed, these authors found that, while the reporting of demographic rate uncertainty is common for matrix population models, this reporting is inconsistent and often incomplete. Thus, when variance decomposition is applied to these models, errors in estimates of vital rates are propagated through estimates of λ_t. For instance, if estimation error in survival or reproduction rates is comparable to temporal fluctuations, then it may be challenging to tease apart the sources of variance in λ_t. In addition, estimating $\mathrm{Var}(\lambda_t)$ requires long-term demographic studies. However, available matrix population model studies are often too short to capture long-term fluctuations (Crone et al., 2013).

We also want to note that our results do not focus on the magnitude of ϵ, which corresponds to the size of perturbations. In the derivations, ϵ is a scaling parameter that allows us to separate the first and second order effects. However, in real ecological systems the size of perturbations can play an important role (Miller et al., 2012). Factors such as vital rate elasticities (Kajin et al., 2025), density-dependent trade-offs (Jaggi et al., 2024b), and demographic buffering (Gascoigne et al., 2025) determine how environmental variation translates into realized variability in survival, growth, and reproduction. Demographic mechanisms may dampen or amplify the effective magnitude of ϵ.

Our framework provides an exact and conceptually transparent decomposition of temporal variation in population growth rate into contributions from vital-rate variability and transient population structure. By unifying stochastic demography with transient dynamics, this approach clarifies when demographic memory is expected to amplify or dampen environmental variability and how these effects depend on life-history strategy and covariance among rates. Unlike retrospective approaches (Knape et al., 2023; Koons et al., 2016), our method requires only temporally replicated demographic models and is therefore well suited for comparative

analyses, cases where long time series of demographic data are not yet available, scenario testing, and forecasting under alternative environmental regimes. As long-term demographic datasets continue to accumulate and are increasingly used to inform management and conservation decisions, this approach offers a robust tool to disentangle extrinsic environmental forcing from intrinsic population responses, and to identify when transient dynamics are likely to play a dominant role in shaping population trajectories.

Table 2: Notation and definitions. Some operators are provided in the first block, and then variables are listed below. We employ the convention for matrix mathematics (following Caswell 2001 and others) wherein vectors are named with lower-case boldface English letters, and matrices are named with upper-case boldface English letters.

Notation	Formula and/or meaning
	Operators
$\mathbf{e}$	A vector where all entries are 1.
$(\mathbf{x}, \mathbf{y})$	The inner product of vectors $\mathbf{x}$ and $\mathbf{y}$.
$(\mathbf{e}, \mathbf{x})$	The inner product of $\mathbf{e}$ and $\mathbf{x}$ is equivalent to the sum of the entries in the vector $\mathbf{x}$.
$\mathcal{E}[X]$	Expected value of X.
	Other parameters and variables
$\mathbf{A}_t$	The population projection matrix containing the vital rates experienced by the focal population from time $t-1$ to time t.
$\overline{\mathbf{A}}$	The population projection matrix long-term mean vital rates experienced by the focal population.
$\mathbf{H}_t$	The matrix of random deviations to the entries of $\overline{\mathbf{A}}$ that give rise to $\mathbf{A}_t$.
$\mathbf{w}_t$	The population structure vector at time t.
$\overline{\mathbf{w}}$	Long-term average population structure vector.
$\mathbf{z}_t$	Vector of deviations between $\mathbf{w}_t$ and $\overline{\mathbf{w}}$.
ϵ	Parameter controlling the relative size of the deviations to $\overline{\mathbf{w}}$ and $\overline{\mathbf{A}}$.
λ_t	Population growth rate from time $t-1$ to time t.
λ_d	Deterministic population growth rate of a population growing according to $\overline{\mathbf{A}}$, calculated as the leading eigenvalue of $\overline{\mathbf{A}}$.
Δ_Z	Contribution to λ_t from the mean vital rates acting on the deviation in population structure, defined as $\left(\mathbf{e}, \overline{\mathbf{A}}\mathbf{z}_{t-1}\right)$.
Δ_R	Contribution to λ_t from the deviations in vital rates acting on the mean population structure, defined as $(\mathbf{e}, \mathbf{H}_t\overline{\mathbf{w}})$.
Δ_{ZR}	Contribution to λ_t from the deviations in vital rates acting on the deviation in population structure, defined as $(\mathbf{e}, \mathbf{H}_t\mathbf{z}_{t-1})$.

References

Bienvenu, F., & Legendre, S. (2015). A new approach to the generation time in matrix population models. *American Naturalist*, *185*, 834–843. https://doi.org/10.1086/681104

Cant, J. I., Hernandez, C. M., Koons, D., Hodgson, D. J., Qi, M., Hector, A., Stott, I., & Salguero-Gomez, R. (2025). Life-history variation mediates the importance of population structure to the short-term dynamics of plant populations worldwide.

Caswell, H. (1989). Analysis of life table response experiments: Decomposition of effects on population growth rate. *Ecological Modelling*, *46*, 221–237. https://doi.org/10.1016/0304-3800(89)90019-7

Caswell, H. (2001). *Matrix population models* (2nd ed.). Sinauer Associates.

Caswell, H. (2007). Sensitivity analysis of transient population dynamics. *Ecology letters*, *10*(1), 1–15.

Caswell, H. (2019). *Sensitivity analysis: Matrix methods in demography and ecology*. Springer Nature.

Chiang, F., Mazdiyasni, O., & AghaKouchak, A. (2021). Evidence of anthropogenic impacts on global drought frequency, duration, and intensity. *Nature communications*, *12*(1), 2754.

Coulson, T., Catchpole, E. A., Albon, S. D., Morgan, B. J. T., Pemberton, J. M., Clutton-Brock, T. H., Crawley, M. J., & Grenfell, B. T. (2001). Age, sex, density, winter weather, and population crashes in Soay sheep. *Science*, *292*(5521), 1528–1531. https://doi.org/10.1126/science.292.5521.1528

Crone, E. E., Ellis, M. M., Morris, W. F., Stanley, A., Bell, T., Bierzychudek, P., Ehrlen, J., Kaye, T. N., Knight, T. M., Lesica, P., et al. (2013). Ability of matrix models to explain the past and predict the future of plant populations. *Conservation Biology*, *27*(5), 968–978.

Crone, E. E., Menges, E. S., Ellis, M. M., Bell, T., Bierzychudek, P., Ehrlén, J., Kaye, T. N., Knight, T. M., Lesica, P., Morris, W. F., Oostermeijer, G., Quintana-Ascencio, P. F., Stanley, A., Ticktin, T., Valverde, T., & Williams, J. L. (2011). How do plant ecologists use matrix population models? *Ecology Letters*, *14*(1), 1–8. https://doi.org/10.1111/j.1461-0248.2010.01540.x

De Kroon, H., Van Groenendael, J., & Ehrlén, J. (2000). Elasticities: A review of methods and model limitations. *Ecology*, *81*(3), 607–618.

Dobson, F. S., Koons, D. N., Saraux, C., Tamian, A., Oli, M. K., & Viblanc, V. A. (2024). The demographic basis of population growth: A 32-year transient Life Table Response Experiment. *Ecology Letters*, *27*(12), e14512. https://doi.org/10.1111/ele.14512

Ellis, M. M., & Crone, E. E. (2013). The role of transient dynamics in stochastic population growth for nine perennial plants. *Ecology*, *94*(8), 1681–1686. https://doi.org/10.1890/13-0028.1

Ellner, S. P., Childs, D. Z., & Rees, M. (2016). *Data-driven modelling of structured populations: A practical guide to the integral projection model*. Springer International Publishing. https://doi.org/10.1007/978-3-319-28893-2_1

Francis, T. B., Abbott, K. C., Cuddington, K., Gellner, G., Hastings, A., Lai, Y.-C., Morozov, A., Petrovskii, S., & Zeeman, M. L. (2021). Management implications of long transients in ecological systems. *Nature Ecology & Evolution*, *5*(3), 285–294.

Fröborg, H., & Eriksson, O. (2003). Predispersal seed predation and population dynamics in the perennial understorey herb actaea spicata. *Canadian Journal of Botany*, *81*(11), 1058–1069. https://doi.org/10.1139/b03-099

Gascoigne, S. J., Kajin, M., Tuljapurkar, S., Santos, G. S., Compagnoni, A., Steiner, U. K., Vinton, A. C., Jaggi, H., Sepil, I., & Salguero-Gómez, R. (2025). Structured demographic buffering: A framework to explore the environmental components and demographic mechanisms underlying demographic buffering. *Ecology Letters*, *28*(2), e70066.

Gascoigne, S. J., Rolph, S., Sankey, D., Nidadavolu, N., Stell Pičman, A. S., Hernández, C. M., Philpott, M. E., Salam, A., Bernard, C., Fenollosa, E., et al. (2023). A standard protocol to report discrete stage-structured demographic information. *Methods in Ecology and Evolution*, *14*(8), 2065–2083.

Godoy, O., & Levine, J. M. (2014). Phenology effects on invasion success: Insights from coupling field experiments to coexistence theory. *Ecology*, *95*(3), 726–736.

Greenberg, D. A., & Green, D. M. (2013). Effects of an invasive plant on population dynamics in toads. *Conservation Biology*, *27*(5), 1049–1057. https://doi.org/https://doi.org/10.1111/cobi.12078

Haridas, C., & Tuljapurkar, S. (2005). Elasticities in variable environments: Properties and implications. *The American Naturalist*, *166*(4), 481–495.

Hastings, A. (2004). Transients: The key to long-term ecological understanding? *Trends in ecology & evolution*, *19*(1), 39–45.

Hastings, A., Abbott, K. C., Cuddington, K., Francis, T., Gellner, G., Lai, Y.-C., Morozov, A., Petrovskii, S., Scranton, K., & Zeeman, M. L. (2018). Transient phenomena in ecology. *Science*, *361*(6406), eaat6412.

Heppell, S. S., Caswell, H., & Crowder, L. B. (2000). Life histories and elasticity patterns: Perturbation analysis for species with minimal demographic data. *Ecology*, *81*(3), 654–665.

Hernández, C. M., Ellner, S. P., Adler, P. B., Hooker, G., & Snyder, R. E. (2023). An exact version of life table response experiment analysis, and the r package exactltre. *Methods in Ecology and Evolution*, *14*, 939–951. https://doi.org/10.1111/2041-210X.14065

Hone, J., Duncan, R. P., & Forsyth, D. M. (2010). Estimates of maximum annual population growth rates (rm) of mammals and their application in wildlife management. *Journal of Applied Ecology*, *47*(3), 507–514.

Hostetler, J. A., Kneip, E., Van Vuren, D. H., & Oli, M. K. (2012). Stochastic population dynamics of a montane ground-dwelling squirrel. *PloS one*, *7*(3), e34379.

Houston, A. I., & McNamara, J. M. (1990). The effect of environmental variability on growth. *Oikos*, 15–20.

Jaggi, H., Steinsaltz, D., & Tuljapurkar, S. (2024a). Temporal variability can promote migration between habitats. *Theoretical Population Biology*, *158*, 195–205.

Jaggi, H., Tuljapurkar, S., Gascoigne, S. J., Zuo, W., Kajin, M., & Salguero-Gómez, R. (2025). Transient dynamics and nonlinear fitness: A unified matrix approach to press and pulse perturbation. *BioRxiv*.

Jaggi, H., Zuo, W., Kentie, R., Gaillard, J.-M., Coulson, T., & Tuljapurkar, S. (2024b). Density dependence shapes life-history trade-offs in a food-limited population. *Ecology Letters*, *27*(11), e14551.

Jiang, S., Jaggi, H., Zuo, W., Oli, M. K., Coulson, T., Gaillard, J.-M., & Tuljapurkar, S. (2022). Reproductive dispersion and damping time scale with life-history speed. *Ecology Letters*, *25*(9), 1999–2008.

Johnson, G. C., & Lyman, J. M. (2020). Warming trends increasingly dominate global ocean. *Nature Climate Change*, *10*(8), 757–761.

Kajin, M., Tuljapurkar, S., Zuo, W., Jaggi, H., Gascoigne, S., & Salguero-Gómez, R. (2025). Second-order elasticities for ecology and evolution: Unravelling nonlinear fitness responses to perturbations. *bioRxiv*, 2025–04.

Knape, J., Paquet, M., Arlt, D., Kačergytė, I., & Pärt, T. (2023). Partitioning variance in population growth for models with environmental and demographic stochasticity. *Journal of Animal Ecology*, *92*(10), 1979–1991. https://doi.org/10.1111/1365-2656.13990

Koons, D. N., Iles, D. T., Schaub, M., & Caswell, H. (2016). A life-history perspective on the demographic drivers of structured population dynamics in changing environments. *Ecology Letters*, *19*(9), 1023–1031. https://doi.org/10.1111/ele.12628

Koons, D. N., Rockwell, R. F., & Grand, J. B. (2006). Population Momentum: Implications for Wildlife Management. *Journal of Wildlife Management*, *70*(1), 19–26. https://doi.org/10.2193/0022-541X(2006)70[19:PMIFWM]2.0.CO;2

Levine, J. M., HilleRisLambers, J., Petry, W. K., Usinowicz, J., & Crowther, T. W. (2024). Demographic but not competitive time lags can transiently amplify climate-induced changes in vegetation carbon storage. *Global Change Biology*, *30*(8), e17432.

Lindell, T., Ehrlén, J., & Dahlgren, J. P. (2022). Weather-driven demography and population dynamics of an endemic perennial plant during a 34-year period. *Journal of Ecology*, *110*(3), 582–592. https://doi.org/https://doi.org/10.1111/1365-2745.13821

Maldonado-Chaparro, A. A., Blumstein, D. T., Armitage, K. B., & Childs, D. Z. (2018). Transient LTRE analysis reveals the demographic and trait-mediated processes that buffer population growth. *Ecology Letters*, *21*(11), 1693–1703. https://doi.org/10.1111/ele.13148

McDonald, J. L., Stott, I., Townley, S., & Hodgson, D. J. (2016). Transients drive the demographic dynamics of plant populations in variable environments. *Journal of Ecology*, *104*(2), 306–314. https://doi.org/10.1111/1365-2745.12528

Menges, E. S., Ascencio, P. F. Q., Weekley, C. W., & Gaoue, O. G. (2006). Population viability analysis and fire return intervals for an endemic florida scrub mint. *Biological conservation*, *127*(1), 115–127.

Metz, J. A. J., Nisbet, R. M., & Geritz, S. A. H. (1992). How should we define 'fitness' for general ecological scenarios? *Trends in Ecology and Evolution*, *7*(6), 198–202.

Miller, A., Reilly, D., Bauman, S., & Shea, K. (2012). Interactions between frequency and size of disturbance affect competitive outcomes. *Ecological research*, *27*(4), 783–791.

Morozov, A., Feudel, U., Hastings, A., Abbott, K. C., Cuddington, K., Heggerud, C. M., & Petrovskii, S. (2024). Long-living transients in ecological models: Recent progress, new challenges, and open questions. *Physics of Life Reviews*, *51*, 423–441.

Oldfather, M. F., & Ackerly, D. D. (2019). Microclimate and demography interact to shape stable population dynamics across the range of an alpine plant. *New Phytologist*, *222*(1), 193–205. https://doi.org/https://doi.org/10.1111/nph.15565

Paniw, M., James, T. D., Ruth Archer, C., Römer, G., Levin, S., Compagnoni, A., Che-Castaldo, J., Bennett, J. M., Mooney, A., Childs, D. Z., Ozgul, A., Jones, O. R., Burns, J. H., Beckerman, A. P., Patwary, A., Sanchez-Gassen, N., Knight, T. M., & Salguero-Gómez, R. (2021). The myriad of complex demographic responses of terrestrial mammals to climate change and gaps of knowledge: A global analysis. *Journal of Animal Ecology*, *90*(6), 1398–1407. https://doi.org/10.1111/1365-2656.13467

Pilowsky, J. A., & Dahlgren, J. P. (2020). Incorporating the temporal autocorrelation of demographic rates into structured population models. *Oikos*, *129*(2), 238–248.

Robey, A. J., Kummel, M. T., & Vasseur, D. A. (2025). Temporal autocorrelation increases temperature-driven extinction risk by clustering stressful conditions. *bioRxiv*, 2025–07.

Rudgers, J. A., & Hoeksema, J. D. (2003). Inter-annual variation in above-and belowground herbivory on a native, annual legume. *Plant Ecology*, *169*(1), 105–120. https://doi.org/10.1023/A:1026221602968

Salguero-Gómez, R., Jones, O. R., Archer, C. R., Bein, C., de Buhr, H., Farack, C., Gottschalk, F., Hartmann, A., Henning, A., Hoppe, G., Römer, G., Ruoff, T., Sommer, V., Wille, J., Voigt, J., Zeh, S., Vieregg, D., Buckley, Y. M., Che-Castaldo, J., ... Vaupel, J. W. (2016). COMADRE: A global data base of animal demography. *Journal of Animal Ecology*, *85*(2), 371–384. https://doi.org/10.1111/1365-2656.12482

Salguero-Gómez, R., Jones, O. R., Archer, C. R., Buckley, Y. M., Che-Castaldo, J., Caswell, H., Hodgson, D., Scheuerlein, A., Conde, D. A., Brinks, E., Buhr, H., Farack, C., Gottschalk, F., Hartmann, A., Henning, A., Hoppe, G., Römer, G., Runge, J., Ruoff, T., ... Vaupel, J. W. (2015). The COMPADRE plant matrix database: An open online repository for plant demography. *Journal of Ecology*, *103*, 202–218. https://doi.org/10.1111/1365-2745.12334

Sibly, R. M., & Hone, J. (2002). Population growth rate and its determinants: An overview. *Philosophical Transactions of the Royal Society of London. Series B: Biological Sciences*, *357*(1425), 1153–1170.

Simmonds, E. G., & Jones, O. R. (2024). Uncertainty propagation in matrix population models: Gaps, importance and guidelines. *Methods in Ecology and Evolution*, *15*(2), 427–438.

Stott, I., Townley, S., Carslake, D., & Hodgson, D. J. (2010). On reducibility and ergodicity of population projection matrix models. *Methods in Ecology and Evolution*, *1*(3), 242–252. https://doi.org/10.1111/j.2041-210X.2010.00032.x

Stott, I., Townley, S., & Hodgson, D. J. (2011). A framework for studying transient dynamics of population projection matrix models. *Ecology Letters*, *14*(9), 959–970. https://doi.org/10.1111/j.1461-0248.2011.01659.x

Summers, J., Cosgrove, E. J., Bowman, R., Fitzpatrick, J. W., & Chen, N. (2024). Density dependence maintains long-term stability despite increased isolation and inbreeding in the Florida Scrub-Jay. *Ecology Letters*, *27*(12), e14483. https://doi.org/10.1111/ele.14483

Sutherland, W. J., Freckleton, R. P., Godfray, H. C. J., Beissinger, S. R., Benton, T., Cameron, D. D., Carmel, Y., Coomes, D. A., Coulson, T., Emmerson, M. C., et al. (2013). Identification of 100 fundamental ecological questions. *Journal of Ecology*, *101*(1), 58–67.

Sutherland, W. J., & Norris, K. (2002). Behavioural models of population growth rates: Implications for conservation and prediction. *Philosophical Transactions of the Royal Society of London. Series B: Biological Sciences*, *357*(1425), 1273–1284.

Thomas, M. B. (1999). Ecological approaches and the development of "truly integrated" pest management. *Proceedings of the National Academy of Sciences*, *96*(11), 5944–5951.

Tuljapurkar, S. (1990). *Population dynamics in variable environments*. Springer.

Tuljapurkar, S., & Haridas, C. (2006). Temporal autocorrelation and stochastic population growth. *Ecology letters*, *9*(3), 327–337.

Tuljapurkar, S., Horvitz, C. C., & Pascarella, J. B. (2003). The many growth rates and elasticities of populations in random environments. *The American Naturalist*, *162*(4), 489–502.

Vázquez, D. P., Gianoli, E., Morris, W. F., & Bozinovic, F. (2017). Ecological and evolutionary impacts of changing climatic variability. *Biological Reviews*, *92*(1), 22–42.

Vélez-Espino, L. A., Ford, J. K. B., Araujo, H., Ellis, G., Parken, C., & Balcomb, K. (2014). *Comparative demography and viability of northeastern pacific resident killer whale populations at risk*. Fisheries; Oceans Canada= Pêches et océans Canada.

Wiedenmann, J., Fujiwara, M., & Mangel, M. (2009). Transient population dynamics and viable stage or age distributions for effective conservation and recovery. *Biological Conservation*, *142*(12), 2990–2996.

Appendices

S1 Contribution of population structure to population growth rate

To illustrate the importance of population structure, we compare projections from structured matrix population models with those from unstructured models obtained by collapsing each matrix to a single survival and fertility rate. Although both models experience the same sequence of environmental variation, the rates differ between unstructured and structured population growth rates as well as realized population sizes. One of the reasons is that the unstructured models assumes that the population is close to stable stage distribution, thereby ignoring the contribution of population structure. As shown in Figure S.1, this simplification can lead to substantial discrepancies in both realized growth rates and population size trajectories. We want to note that this collapse is not well-defined for Orcas because their matrices exhibit near-stasis in some stages (i.e., transition probabilities equal to one) which makes the comparison unreliable. Hence we excluded Orcas for comparison between structured snd unstructured population size and growth rate in the figure below.

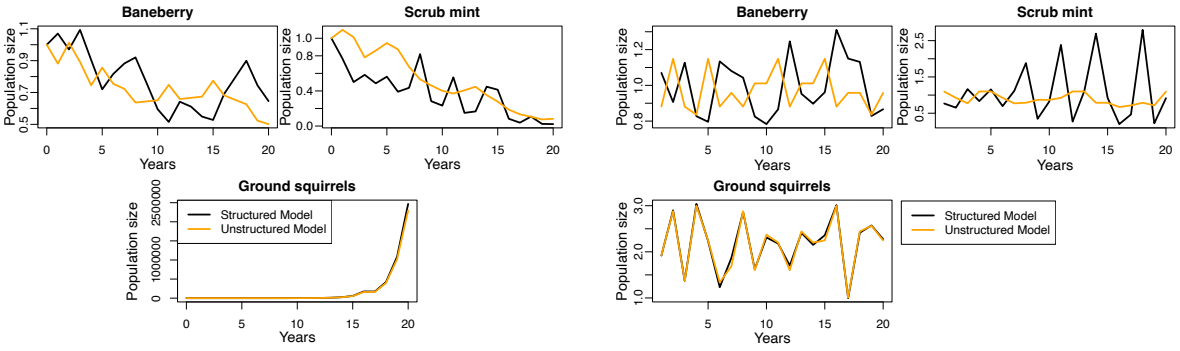

(a) Comparison of population size trajectories.

(b) Comparison of population growth rates.

Figure S.1: Comparison between structured and unstructured models. The left panels compare population size trajectories and the right panels compare realized population growth rates between unstructured model (yellow) and structured model (black). We compare these across three species: baneberry, scrub mint, and ground squirrel in both the panels.

S2 Decomposition for the growth rate λ_t

In this section, we decompose the growth rate as shown in the main manuscript, arriving at Equation (5). The population projection matrix $\mathbf{A}_t$ at time t describes the transitions of individuals between different life (st)ages or size classes at each time t.

As discussed in Tuljapurkar (1990), the population structure at time t is denoted $\mathbf{w}_t$ and changes over time as

$$\mathbf{w}_t = \frac{\mathbf{A}_t\,\mathbf{w}_{t-1}}{\lambda_t}, \quad \lambda_t = (\mathbf{e}, \mathbf{A}_t\mathbf{w}_{t-1}), \tag{S1}$$

where $\mathbf{e}$ is a vector with all elements equal to 1, and (.) denotes the scalar product. Since $\mathbf{w}_t$ is population structure (proportion of individuals in each age/stage), $(\mathbf{e}, \mathbf{w}_t) = 1$.

Equation (S1) shows that the stage distribution at time t ($\mathbf{w}_t$) is obtained by projecting forward the previous population structure $\mathbf{w}_{t-1}$, scaled by the growth rate λ_t. Here, λ_t tracks changes in total population abundance from time $(t-1)$ to time t.

We express the time-varying matrix $\mathbf{A}_t$ as a sum of the mean projection matrix, $\overline{\mathbf{A}}$, and random perturbations to the underlying demographic rates:

$$\mathbf{A}_t = \overline{\mathbf{A}} + \epsilon\mathbf{H}_t, \quad \mathcal{E}[\mathbf{H}_t] = 0, \tag{S2}$$

where $\mathbf{H}_t$ represents the random deviations in demographic rates with mean zero, $\mathcal{E}$ denotes the expectation, and ϵ scales the magnitude of the fluctuations.

S3 Interlude on the Average Matrix

The dominant eigenvalue of $\overline{\mathbf{A}}$ is λ_d, with the corresponding right eigenvector $\mathbf{u}$ (the stable population structure) and $\mathbf{v}$ (the reproductive value). Normalize so that $(\mathbf{e}, \mathbf{u}) = 1$ and $(\mathbf{v}, \mathbf{u}) = 1$. Thus we have:

$$\overline{\mathbf{A}}\mathbf{u} = \lambda_d \mathbf{u} \iff \lambda_d = (\mathbf{e}, \overline{\mathbf{A}}\mathbf{u}) \iff \mathbf{u} = \frac{\overline{\mathbf{A}}\mathbf{u}}{(\mathbf{e}, \overline{\mathbf{A}}\mathbf{u})}. \tag{S3}$$

Next, we introduce the projection operator

$$\mathbf{P} = \mathbf{u}\,\mathbf{v}^T = \mathbf{P}^2. \tag{S4}$$

The matrix $\mathbf{P}$ projects the system in the asymptotic direction defined by the dominant eigenvectors $\mathbf{u}$ and $\mathbf{v}$ (Tuljapurkar et al., 2023). By the Perron-Frobenius theorem (Caswell, 2012; Tuljapurkar et al., 2023), we can decompose the mean projection matrix ($\overline{\mathbf{A}}$) into two components:

$$\overline{\mathbf{A}} = \lambda_d(\mathbf{P} + \mathbf{Q}), \tag{S5}$$

where $\mathbf{P}$ captures the asymptotic dynamics and $\mathbf{Q}$ governs the transient deviations. Note that $\mathbf{P}$ and $\mathbf{Q}$ are orthogonal, that is, $\mathbf{PQ} = 0$. Normalizing by λ_d:

$$\mathbf{B} = \frac{\overline{\mathbf{A}}}{\lambda_d} = (\mathbf{P} + \mathbf{Q}), \tag{S6}$$

$$\mathbf{B}^m = \mathbf{P} + \mathbf{Q}^m, \text{ for } m \geq 1, \tag{S7}$$

the effect of $\mathbf{Q}$ decays over time as:

$$\mathbf{Q}^m \to 0 \propto \rho^m, \text{ with } 0 < \rho < 1, \tag{S8}$$

where ρ is the asymptotic damping rate and determines the rate at which populations converge to a stable stage distribution. Thus, the projection operator $\mathbf{P}$ represents the projection of the system along the direction associated with λ_d. In other words, $\mathbf{P}$ is the part of $\overline{\mathbf{A}}$ that is associated with the asymptotic dynamics whereas $\mathbf{Q}$ is the part of $\overline{\mathbf{A}}$ that is orthogonal to $\mathbf{P}$,

and associated with transient dynamics. Jiang et al. (2022) showed that

$$\rho \propto \frac{1}{T_c} \text{ with } T_c = \text{ cohort generation time.}$$

Therefore, we can expect that species with a long generation time will exhibit slower decay of transient dynamics.

S4 Decomposition continued

To simplify, we scale equation (S2) by λ_d

$$\frac{\mathbf{A}_t}{\lambda_d} = \frac{\overline{\mathbf{A}}}{\lambda_d} + \epsilon \frac{\mathbf{H}_t}{\lambda_d}$$

Substituting equation (S6) to the equation above, we get

$$\frac{\mathbf{A}_t}{\lambda_d} = \mathbf{B} + \epsilon \mathbf{G}_t, \text{ where } \mathbf{G}_t = \frac{\mathbf{H}_t}{\lambda_d} \quad \text{and } \mathcal{E}[\mathbf{G}_t] = 0. \tag{S9}$$

Then we rewrite the age-structure iteration in equation (S1) as the equivalent expression

$$\mathbf{w}_t = \frac{(\mathbf{B} + \epsilon \mathbf{G}_t)\, \mathbf{w}_{t-1}}{\eta_t}, \quad \eta_t = \frac{\lambda_t}{\lambda_d} = (\mathbf{e}, (\mathbf{B} + \epsilon \mathbf{G}_t)\mathbf{w}_{t-1})\,. \tag{S10}$$

To separate the average dynamics from fluctuations, the population structure at time t is now decomposed as a sum:

$$\mathbf{w}_t = \overline{\mathbf{w}} + \epsilon \mathbf{z}_t \tag{S11}$$

where $\mathbf{z}_t$ represents the deviations from the stable stage distribution $\mathbf{u}$. As $\epsilon \to 0$, the average population structure $\overline{\mathbf{w}} \to \mathbf{u}$. Thus, to leading order (*i.e.*, $\epsilon \to 0$):

$$\overline{\mathbf{w}} = \frac{\mathbf{B}\overline{\mathbf{w}}}{(\mathbf{e}, \mathbf{B}\overline{\mathbf{w}})}, \tag{S12}$$

which means that to this order $\overline{\mathbf{w}}$ is the (dominant) right eigenvector of $\mathbf{B}$ which is also the right eigenvector of the average matrix $\overline{\mathbf{A}}$, so $\overline{\mathbf{w}} = \mathbf{u}$.

Using the expansion in equation (S11) and keeping terms to order ϵ, we get,

$$
\begin{aligned}
(\mathbf{B}+\epsilon\mathbf{G}_t)\,\mathbf{w}_{t-1} =& (\mathbf{B}+\epsilon\mathbf{G}_t)\,(\overline{\mathbf{w}}+\epsilon\mathbf{z}_{t-1}), && \text{(S13)}\\
=& \mathbf{B}\overline{\mathbf{w}}+\epsilon\mathbf{B}\mathbf{z}_{t-1}+\epsilon\mathbf{G}_t\overline{\mathbf{w}}+O(\epsilon^2), && \text{(S14)}\\
\approx& \mathbf{B}\mathbf{u}+\epsilon\mathbf{B}\mathbf{z}_{t-1}+\epsilon\mathbf{G}_t\overline{\mathbf{w}} && \text{(S15)}\\
=& \mathbf{u}+\epsilon\mathbf{B}\mathbf{z}_{t-1}+\epsilon\mathbf{G}_t\overline{\mathbf{w}} && \text{(S16)}
\end{aligned}
$$

Similarly substituting (S11) into the equation for η_t to the same order

$$
\begin{aligned}
\eta_t =& (\mathbf{e},\mathbf{B}\overline{\mathbf{w}})+\epsilon\,(\mathbf{e},\mathbf{B}\mathbf{z}_{t-1})+\epsilon\,(\mathbf{e},\mathbf{G}_t\overline{\mathbf{w}}) && \text{(S17)}\\
=& (\mathbf{e},\mathbf{B}\mathbf{u})+\epsilon\,(\mathbf{e},\mathbf{B}\mathbf{z}_{t-1})+\epsilon\,(\mathbf{e},\mathbf{G}_t\overline{\mathbf{w}}) && \text{(S18)}\\
=& (\mathbf{e},\mathbf{u})+\epsilon\,(\mathbf{e},\mathbf{B}\mathbf{z}_{t-1})+\epsilon\,(\mathbf{e},\mathbf{G}_t\overline{\mathbf{w}}) && \text{(S19)}\\
=& 1+\epsilon\,(\mathbf{e},\mathbf{B}\mathbf{z}_{t-1})+\epsilon\,(\mathbf{e},\mathbf{G}_t\overline{\mathbf{w}}) && \text{(S20)}\\
=& 1+\epsilon\alpha_t && \text{(S21)}
\end{aligned}
$$

where $\alpha_t = (\mathbf{e},(\mathbf{B}\mathbf{z}_{t-1}+\mathbf{G}_t\overline{\mathbf{w}}))$ is a scalar.

The above expressions give us the numerator and denominator for equation (S10):

$$
\begin{aligned}
\mathbf{w}_t =& \frac{(\mathbf{B}+\epsilon\mathbf{G}_t)\,\mathbf{w}_{t-1}}{\eta_t} && \text{(S22)}\\
=& (\mathbf{u}+\epsilon\mathbf{B}\mathbf{z}_{t-1}+\epsilon\mathbf{G}_t\overline{\mathbf{w}})\,\eta_t^{-1} && \text{(S23)}\\
=& (\mathbf{u}+\epsilon\mathbf{B}\mathbf{z}_{t-1}+\epsilon\mathbf{G}_t\overline{\mathbf{w}})\,(1+\epsilon\alpha_t)^{-1},\ \text{take binomial approximation} && \text{(S24)}\\
=& (\mathbf{u}+\epsilon\mathbf{B}\mathbf{z}_{t-1}+\epsilon\mathbf{G}_t\overline{\mathbf{w}})\,(1-\epsilon\alpha_t),\ \text{expand to first order} && \text{(S25)}\\
\approx& \mathbf{u}+\epsilon\mathbf{B}\mathbf{z}_{t-1}+\epsilon\mathbf{G}_t\overline{\mathbf{w}}-\epsilon\alpha_t\mathbf{u} && \text{(S26)}\\
\mathbf{w}_t =& \mathbf{u}+\epsilon\,(\mathbf{B}\mathbf{z}_{t-1}+\mathbf{G}_t\overline{\mathbf{w}}-\alpha_t\mathbf{u}) && \text{(S27)}
\end{aligned}
$$

But we know $\mathbf{w}_t = \overline{\mathbf{w}}+\epsilon\mathbf{z}_t = \mathbf{u}+\epsilon\mathbf{z}_t$. Comparing this with equation (S27), we get the

dynamics of deviations $\mathbf{z}_t$ as:

$$\mathbf{z}_t = \mathbf{B}\mathbf{z}_{t-1} + \mathbf{G}_t\overline{\mathbf{w}} - \alpha_t\mathbf{u} \tag{S28}$$

$$= \mathbf{B}\mathbf{z}_{t-1} + \mathbf{G}_t\overline{\mathbf{w}} - (\mathbf{e}, (\mathbf{B}\mathbf{z}_{t-1} + \mathbf{G}_t\overline{\mathbf{w}}))\,\mathbf{u} \tag{S29}$$

$$= \mathbf{B}\mathbf{z}_{t-1} + \mathbf{G}_t\overline{\mathbf{w}} - \mathbf{e}^T(\mathbf{B}\mathbf{z}_{t-1} + \mathbf{G}_t\overline{\mathbf{w}})\mathbf{u} \tag{S30}$$

$$= \left(\mathbf{I} - \mathbf{e}^T\mathbf{u}\right)(\mathbf{B}\mathbf{z}_{t-1} + \mathbf{G}_t\overline{\mathbf{w}}) \tag{S31}$$

$$\boxed{\mathbf{z}_t = \mathbf{K}\,(\mathbf{B}\mathbf{z}_{t-1} + \mathbf{G}_t\overline{\mathbf{w}})} \tag{S32}$$

where $\mathbf{K} = 1 - \mathbf{u}\,\mathbf{e}^T$.

We also know that $\lambda_t = \lambda_d\eta_t$ from equation (S10). Substituting the equation for η_t in (S21), we get

$$\lambda_t = \lambda_d\,(1 + \epsilon\,(\mathbf{e}, \mathbf{B}\mathbf{z}_{t-1}) + \epsilon\,(\mathbf{e}, \mathbf{G}_t\overline{\mathbf{w}})) \tag{S33}$$

$$\boxed{\lambda_t = \lambda_d + \epsilon\Delta_Z + \epsilon\Delta_R} \tag{S34}$$

where $\Delta_Z = \lambda_d\,(\mathbf{e}, \mathbf{B}\mathbf{z}_{t-1})$ results from fluctuations in population structure and $\Delta_R = \lambda_d\,(\mathbf{e}, \mathbf{G}_t\mathbf{u})$ captures fluctuations in demographic rates. Thus, we decompose λ_t into the deterministic component λ_d and two first-order contributions from fluctuation in population structure (Δ_Z) and from fluctuation in demographic rates (Δ_R).

S5 Expectation for λ_t

We have assumed that $\mathcal{E}[\mathbf{H}_t] = 0 = \mathcal{E}[\mathbf{G}_t]$ and to order ϵ we have $\mathcal{E}[\mathbf{z}_t] = 0$. So to leading order,

$$\begin{aligned}\mathcal{E}[\lambda_t] &= \lambda_d,\\ \mathcal{E}[\Delta_Z] &= 0,\\ \mathcal{E}[\Delta_R] &= 0.\end{aligned} \tag{S35}$$

S6 Variance for λ_t

From the previous expressions we approximate the variance in growth rate as:

$$\boxed{\mathrm{Var}(\lambda_t) \approx \mathrm{Var}(\Delta_Z) + \mathrm{Var}(\Delta_R)} \tag{S36}$$

Here,

- The first term represents the variance due to fluctuations in the population structure. These fluctuations capture the accumulated effects of past variation in vital rates.
- The second term represents the variance due to random perturbations in the vital rates (*i.e.* in elements of the population projection matrix) at time t. We have assumed that our population reaches stationarity, meaning that the perturbations are drawn from a distribution that does not depend on t. This implies that the magnitude of variance is the same for every t.
- Note that there may also be a covariance term between Δ_Z and Δ_R. When the perturbations are iid (*i.e.,* independent and identically distributed, drawn from the stationary distribution of perturbations), then $\mathbf{G}_t$ is independent of $\mathbf{z}_{t-1}$ and therefore the covariance term is 0. Otherwise, it may be nonzero.

Thus, the variance in the growth rate λ_t is influenced primarily by the variances in Δ_Z and Δ_R, and their covariance. Next we will further derive for terms in the expression for $\mathrm{Var}(\lambda_t)$ as shown below.

S6.0.1 Derivation of $\mathbf{Var}(\Delta_R)$

We know that $\Delta_R = \lambda_d\left(\mathbf{e}, \mathbf{G}_t\mathbf{u}\right)$ and so

$$\mathrm{Var}[\Delta_R] = \mathcal{E}\left[(\lambda_d \mathbf{e}^T \mathbf{G}_t \mathbf{u})^2\right] \tag{S37}$$

$$= \mathcal{E}\left[(\mathbf{e}^T \mathbf{H}_t \mathbf{u})^2\right], \tag{S38}$$

$$= \mathcal{E}\left[\left(\mathbf{e}^T \otimes \mathbf{e}^T\right)\left(\mathbf{H}_1 \otimes \mathbf{H}_1\right)\left(\mathbf{u} \otimes \mathbf{u}\right)\right], \tag{S39}$$

$$= \left(\mathbf{e}^T \otimes \mathbf{e}^T\right)\mathcal{E}\left[\mathbf{H}_1 \otimes \mathbf{H}_1\right]\left(\mathbf{u} \otimes \mathbf{u}\right), \tag{S40}$$

$$\boxed{\mathrm{Var}[\Delta_R] = \left(\mathbf{e}^T \otimes \mathbf{e}^T\right)\Sigma_1\left(\mathbf{u} \otimes \mathbf{u}\right)} \tag{S41}$$

where $\Sigma_1 = \mathcal{E}\left[\mathbf{H}_1 \otimes \mathbf{H}_1\right]$. In step two of this derivation, we used $\lambda_d \mathbf{G}_t = \mathbf{H}_t$. In step 3, we used the Kronecker product and set $t = 1$; we could have used any t due to stationarity. In step 4, we moved the expectation to the random bit. In steps 5 we identified that the expectation of the Kronecker product of random fluctuations is the var-cov matrix Σ_1 of the fluctuations in the matrix elements.

The analytical insight here is that the variation in λ_t that is contributed by the fluctuations in vital rates is equivalent to the sum of the variance in vital rates weighted by the stable population distribution. The analytical predictions here are:

(1) the effect of varying rates depends on the size of fluctuations, as well as the representation of those sizes in the stable structure.

(2) overall variance in growth rates can be held down by negative correlations between rates.

(3) this component of variance in growth rate does NOT depend on serial correlation.

S6.0.2 Derivation of $\mathbf{Var}(\Delta_Z)$

The variance of $\Delta_Z = \lambda_d\left(\mathbf{e}, \mathbf{B}\mathbf{z}_{t-1}\right)$ is:

$$\mathrm{Var}(\Delta_Z) = \lambda_d^2 \mathcal{E}[(\mathbf{e}^T \mathbf{B}\mathbf{z}_{t-1})^2].$$

The last term above is

$$\mathcal{E}\left[(\mathbf{e}^T \mathbf{B}\mathbf{z}_{t-1})^2\right] = \mathcal{E}\left[\left(\mathbf{e}^T \otimes \mathbf{e}^T\right)\left(\mathbf{B}\mathbf{z}_{t-1} \otimes \mathbf{B}\mathbf{z}_{t-1}\right)\right]. \tag{S42}$$

We now return to the boxed equation (S32) which we write again here for convenience:

$$\mathbf{z}_t = \mathbf{K}\left(\mathbf{B}\mathbf{z}_{t-1} + \mathbf{G}_t\mathbf{u}\right), \quad \mathbf{K} = 1 - \mathbf{u}\,\mathbf{e}^T.$$

Take Kronecker products and expectations to get:

$$\mathcal{E}\left[\mathbf{z}_t \otimes \mathbf{z}_t\right] = \left[\mathbf{K}\mathbf{B} \otimes \mathbf{K}\mathbf{B}\right]\mathcal{E}\left[\mathbf{z}_{t-1} \otimes \mathbf{z}_{t-1}\right] + \left[\mathbf{K} \otimes \mathbf{K}\right]\left[\mathbf{G}_t \otimes \mathbf{G}_t\right]\left[\mathbf{u} \otimes \mathbf{u}\right]. \tag{S43}$$

Stationarity means that the var-cov of $\mathbf{z}_t$ (*i.e.*, the Kronecker product of $\mathbf{z}_t$ with itself) at t

and $t-1$ are the same, so we can now solve to get:

$$\mathcal{E}\left[\mathbf{z}_t \otimes \mathbf{z}_t\right] = \left[\mathbf{KB} \otimes \mathbf{KB}\right] \mathcal{E}\left[\mathbf{z}_t \otimes \mathbf{z}_t\right] + \left[\mathbf{K} \otimes \mathbf{K}\right] \left[\mathbf{G}_t \otimes \mathbf{G}_t\right] \left[\mathbf{u} \otimes \mathbf{u}\right] \tag{S44}$$

$$\mathcal{E}\left[\mathbf{z}_t \otimes \mathbf{z}_t\right] = \left(\mathbf{I} - \left[\mathbf{KB} \otimes \mathbf{KB}\right]\right)^{-1} \left[\mathbf{K} \otimes \mathbf{K}\right] \mathcal{E}[\mathbf{G}_t \otimes \mathbf{G}_t] \left[\mathbf{u} \otimes \mathbf{u}\right]. \tag{S45}$$

Another segue about K

Recall the projection operator $\mathbf{P} = \mathbf{u}\mathbf{v}^T$ in equation (S4) and the decomposition $\mathbf{B} = \mathbf{P}+\mathbf{Q}$ in equation (S6). Note that $\mathbf{P}$ and $\mathbf{Q}$ are orthogonal ($\mathbf{PQ} = 0$). Using these,

$$\mathbf{Pu} = \mathbf{u}, \tag{S46}$$

$$\mathbf{e}^T\mathbf{P} = \mathbf{v}^T, \tag{S47}$$

$$\mathbf{u}\mathbf{e}^T\mathbf{P} = \mathbf{P}, \tag{S48}$$

$$\mathbf{PK} = \mathbf{P} - \mathbf{u}\,\mathbf{e}^T, \tag{S49}$$

$$\mathbf{QK} = \mathbf{Q}, \tag{S50}$$

$$\mathbf{BK} = \mathbf{P} - \mathbf{u}\,\mathbf{e}^T + \mathbf{Q} = \mathbf{B} - \mathbf{u}\mathbf{e}^T \tag{S51}$$

$$\mathbf{KB} = \mathbf{KP} + \mathbf{KQ} = \mathbf{KQ}, \tag{S52}$$

$$\mathbf{K}^n = \mathbf{K}, n \geq 2, \tag{S53}$$

$$[\mathbf{KQ}]^2 = \mathbf{KQKQ} = \mathbf{KQ}^2. \tag{S54}$$

Finally, for completeness, we return to equation (S45) and show that the strange looking Kronecker product converges:

$$\left[\mathbf{I} - (\mathbf{KB} \otimes \mathbf{KB})\right]^{-1} = \mathbf{I} + \mathbf{KB} \otimes \mathbf{KB} + (\mathbf{KB} \otimes \mathbf{KB})^2 + \ldots, \tag{S55}$$

$$(\mathbf{KB} \otimes \mathbf{KB})^2 = \left[\mathbf{KB} \otimes \mathbf{KB}\right] \left[\mathbf{KB} \otimes \mathbf{KB}\right], \tag{S56}$$

$$= (\mathbf{KB})^2 \otimes (\mathbf{KB})^2, \tag{S57}$$

$$= (\mathbf{KQ}^2) \otimes (\mathbf{KQ}^2), \tag{S58}$$

$$= (\mathbf{K} \otimes \mathbf{K})\,(\mathbf{Q}^2 \otimes \mathbf{Q}^2). \tag{S59}$$

The point here is that the Kronecker product inverse inherits convergence from the powers of $\mathbf{Q}$. Recall equation (S8) and comments after. So the var-cov of $\mathbf{z}_t$ will be larger if convergence

is slower, i.e., will rise with T_c.

Back to the derivation of Var(Δ_Z)

From equation (S42) we have

$$\mathcal{E}\left[(\mathbf{e}^T\mathbf{B}\mathbf{z}_{t-1})^2\right] = \left(\mathbf{e}^T \otimes \mathbf{e}^T\right)\,(\mathbf{B}\otimes\mathbf{B})\,\mathcal{E}\left[\mathbf{z}_t \otimes \mathbf{z}_t\right]. \tag{S60}$$

And we have the var-cov of $\mathbf{z}_t$ from equation (S45).

Therefore, finally, the variance of Δ_Z is:

$$\mathrm{Var}(\Delta_Z) = \lambda_d^2\,\mathcal{E}[(\mathbf{e}^T\mathbf{B}\mathbf{z}_{t-1})^2] \tag{S61}$$

$$\boxed{\mathrm{Var}(\Delta_Z) = \lambda_d^2\left(\mathbf{e}^T \otimes \mathbf{e}^T\right)\,(\mathbf{B}\otimes\mathbf{B})\,\mathcal{E}\left[\mathbf{z}_t \otimes \mathbf{z}_t\right]} \tag{S62}$$

Predictions:

a) The size of fluctuations (in $\mathbf{H}_t$ and thus $\mathbf{G}_t$) affects the fluctuations in $\mathbf{z}_t$ and will carry through to fluctuations in λ_t.

b) Previous work shows that convergence (powers of $\mathbf{Q}$ going to zero) is related to generation time, so based on that we can expect that species with a high generation time will show higher contributions from Δ_Z because of increase in $\mathcal{E}\left[\mathbf{z}_t \otimes \mathbf{z}_t\right]$.

S7 Simulation procedure

To numerically calculate the terms in the decomposition of variance in population growth rate into the terms shown in Equation (S36), we use a simulation procedure. For each simulation, we use an initial population vector that is evenly distributed across classes. To remove any effects of this initial population vector, we use a burn-in period, *i.e.*, simulation time steps that are discarded before calculating the decomposition. The decomposition is then calculated for one time step following the burn-in.

a) We select a population represented by m annual transition matrices (*e.g.*, same grassland plot for m different years). In the case studies presented here, we used populations from the COMADRE and COMPADRE databases (Salguero-Gómez et al., 2015; Salguero-Gómez et al., 2016).

b) We calculate the burn-in time as $100T_g$, where T_g is the generation time of the mean matrix $\overline{\mathbf{A}}$. We calculate the mean survival and fertility matrices by taking the element-wise average of the m **U** and **F** matrices, and use these mean matrices to calculate the generation time. We used the definition of generation time from Bienvenu and Legendre (2015), *i.e.,* the average age difference between parents and offspring.

c) For each of n replicate simulations, we generate a sequence of environments of length $t_{burn-in} + 1$. The m annual transition matrices have equal probabilities of being chosen at each time step. We generate this as a $m \times n$ matrix of environments where each column corresponds to one replicate. We refer to the projection matrix for a given time step t in the environmental sequence for a given replicate i as $\mathbf{A}_{i,t}$.

d) Because our replicates are a finite sample of matrices, we need to correct for the sample mean in the final time step. In other words, it takes an extremely large number of replicate runs to ensure that the mean (across replicates) of the final-time-step $\mathbf{A}_{i,t_{final}}$ matrices would exactly match $\overline{\mathbf{A}}$. To correct for this, we calculate the offset in matrix elements between $\overline{\mathbf{A}}$ and our sample mean, and add this offset to our sampled final-time-step matrices $\mathbf{A}_{i,t_{final}}$.

e) For each replicate run i:

- We run the burn-in time steps, starting from a population with $1/s$ individuals in each size/stage/age class, where s is the number of size/stage/age classes. For each time t, we evaluate $\mathbf{A}_{i,t}\mathbf{w}_{t-1}$. After each iteration, we re-normalize the population vector to the population structure ($\mathbf{w}_t$, where the sum of entries is equal to 1). Because the vital rates are not dependent on population size/density, it is only the relative size of the different size/stage/age classes that matters for driving variation in population growth rate. Therefore, since we are not concerned with the total population size, we re-normalize the population vectors at each time step. This re-normalization avoids numerical errors related to storing large numbers in computing languages such as R.
- For the final time step, we save the environmental matrix ($\mathbf{A}_{i,t_{final}}$), the population structure at the start of the final time step ($\mathbf{w}_{i,t-1}$), and the one-time-step

population growth rate

$(\lambda_{i,t} = \|\mathbf{w}_{i,t}\|_1 / \|\mathbf{w}_{i,t-1}\|_1)$.

f) After all the replicate simulations are run, we have n realizations of λ_t, for which we can calculate Δ_Z and Δ_R according to Equation (S33). Then we calculate the variances of the terms Δ_Z and Δ_R as our contributions to variance in λ_t as shown in Equation (S36).